Food Hydrocolloids for Health 9 (2026) 100273

Contents lists available at ScienceDirect

Food Hydrocolloids for Health

journal homepage: www.elsevier.com/locate/fhfh

Valorization of soybean seed coat pectic fibers as functional food hydrocolloids with anti-obesity activity

Xiaoyi Liu [a,1], Guowei Chen [b,1], Junliang Chen [a,1], Jiahong Huo [a], Hong Yao [a], Maurizio Battino [c,d], Weibin Bai [a,*], Lingmin Tian [a,*]

[a] Department of Food Science and Engineering, International School, College of Life Science and Technology, Jinan University, Guangzhou, China
[b] Weifang Institute of Technology, Weifang, China
[c] Department of Clinical Science, Polytechnic University of Marche, Ancona 60130, Italy
[d] Research Group on Foods, Nutritional Biochemistry and Health, European University of Atlantico, Isabel Torres 21, Santander 39011, Spain

ARTICLE INFO

Keywords:
Glycine max (L.) Merr.
Soybean seed coat
Pectin-rich polysaccharides
Dietary fiber
Obesity
Gut microbiota
Lipid metabolism

ABSTRACT

Soybean seed coats (episperm) are an underutilized byproduct of soybean processing and represent a potential source of pectin-rich dietary fibers. In this study, black soybean seed coat (BSC), yellow soybean seed coat (YSC), and their dietary fiber (DF)-enriched fractions (BSCF and YSCF) were characterized for chemical composition and evaluated for their effects on high-fat diet (HFD)-induced obesity in mice. Monosaccharide composition analysis showed that all samples were dominated by arabinose-, galactose-, rhamnose-, and galacturonic acid–containing polysaccharides, indicating the presence of pectin-like structures rich in rhamnogalacturonan-I domains. Dietary supplementation with soybean seed coat preparations significantly attenuated HFD-induced body weight gain, adiposity, and hepatic steatosis, with BSCF showing the most pronounced effects. Improvements in serum lipid and glucose parameters were accompanied by modulation of hepatic genes related to inflammation and lipid metabolism. Histological analysis confirmed reduced lipid accumulation in liver and adipose tissues. In addition, soybean seed coat supplementation increased gut microbial α-diversity, altered overall microbial community structure, reduced the abundance of inflammation-associated phyla, and modulated several obesity-related genera. Correlation analysis further revealed associations between inflammatory cytokines, lipid metabolism–related genes, and gut microbiota. Overall, these results demonstrate that soybean seed coats, particularly their DF-enriched fractions, are a promising source of pectin-rich hydrocolloids with potential applications in functional foods targeting obesity and metabolic disorders.

1. Introduction

Obesity is a multifactorial metabolic disorder associated with chronic low-grade inflammation, dysregulated lipid handling, and alterations in gut microbiota (Cheng et al., 2022; Le Chatelier et al., 2013; Rajha et al., 2022). As interest grows in natural, food-derived solutions for weight management, plant polysaccharides, especially pectin and pectin-like hydrocolloids, have received increasing attention for their capacity to regulate digestion, lipid absorption, and microbial fermentation (Tian et al., 2016; Tian et al., 2017; Tian et al., 2019).

Soybean seed coats, the episperm removed during soybean processing, represent a substantial yet underutilized biomass. Yellow soybean seed coats (YSC) and black soybean seed coats (BSC) are typically discarded or burned, despite being rich in DFs and structurally complex polysaccharides (Mullin & Xu, 2000; Yang et al., 2014). Emerging compositional evidence, including data from this study, indicates that soybean seed coat fibers contain high levels of arabinose, galactose, rhamnose, and uronic acids, hallmark features of pectic polysaccharides, particularly rhamnogalacturonan-I (Mullin & Xu, 2000). These pectin-rich polysaccharides exhibit functional characteristics similar to other food hydrocolloids—water retention, viscosity development, and fermentability—that may contribute to metabolic health (Tian et al., 2019).

While BSC also contain polyphenols such as anthocyanins (Zhang et al., 2024), the DF-rich fractions obtained after removal of extractable flavonoids (BSCF and YSCF) consist predominantly of structural pectic

* Corresponding authors.
E-mail addresses: baiweibin@163.com (W. Bai), tianlinmin@163.com (L. Tian).
[1] These three authors have contributed equally to this work.

https://doi.org/10.1016/j.fhfh.2026.100273
Received 26 December 2025; Received in revised form 19 February 2026; Accepted 4 March 2026
Available online 5 March 2026

polysaccharides, enabling targeted investigation of DF-specific biological effects. Pectin and related hydrocolloids influence metabolic outcomes through several mechanisms, e.g. modulating gut microbiota, promoting short-chain fatty acids (SCFAs) production (Ju et al., 2025; Méndez-Albiñana et al., 2025; Yüksel et al., 2025).

Although phenolic extracts from soybean seed coats have been previously studied for anti-obesity effects (Hironao et al., 2022), the role of soybean seed coat pectin-like DFs has not been thoroughly examined, particularly in the context of structure–function relationships central to food hydrocolloids research. This study therefore aimed to (i) characterize the biochemical and monosaccharide composition of BSC, YSC, and their corresponding DF fractions, with emphasis on their pectin-rich polysaccharide structures, and (ii) evaluate their ability to mitigate high-fat diet (HFD)-induced obesity, metabolic dysfunction, inflammation, and gut microbiota changes in mice. By integrating polysaccharide composition with physiological outcomes, this work provides a foundation for valorizing soybean seed coat pectins as functional hydrocolloids with anti-obesity potential.

2. Experimental section

2.1. Sample and diet preparation

Both BSC and YSC, sourced from Anhui, China, were milled, passed through an 80-mesh sieve, and divided into two portions: untreated powder and flavonoid-depleted powder obtained through sequential extraction. Briefly, the soybean seed coat flour was first defatted by three consecutive extractions with petroleum ether (1:3 w/v, 24 h each). The defatted powder (1.5 kg) was then extracted three times with acidified 65% ethanol (0.1% trifluoroacetic acid, v/v; 15 L) at 4°C in the dark for 8 h per extraction (Zhang et al., 2024). The resulting residues were lyophilized to obtain the flavonoid-depleted DF fractions, designated BSCF and YSCF.

The experimental diets were formulated based on the D12450H and D12451 diets (Research Diets), with modifications to increase the DF content. Detailed diet compositions are provided in Table 1. In our previous study, a diet containing 3% purified pectin was shown to exert significant physiological effects in mice, providing a reference level for biologically relevant pectin intake (Tian et al., 2016; Tian et al., 2017; Tian et al., 2019). To achieve a comparable ~3% pectin equivalent using whole soybean seed coat materials, which contain pectin as only one component, a substantially higher inclusion level was necessary. Therefore, the BSC, YSC, BSCF, and YSCF diets incorporated 15.66% (w/w) of the respective soybean seed coat materials in place of cellulose in HFD diet, and the control diet (CD) contained 12.99% (w/w) cellulose. This resulted in experimental diets with a higher total DF content than the standard D12450H/D12451 formulations, ensuring that the pectin-rich polysaccharide fraction was present at functionally meaningful levels for biological evaluation.

Table 1
Composition of the experimental diets.

Ingredient (g)	Diet for experimental mice groups					
	CD	HFD	BSC	BSCF	YSC	YSCF
BSC fraction	0	0	15.66	0	0	0
BSCF fraction	0	0	0	15.66	0	0
YSC fraction	0	0	0	0	15.66	0
YSCF fraction	0	0	0	0	0	15.66
Cellulose	12.99	15.66	0	0	0	0
Casein, 80 Mesh	17.31	20.87	20.87	20.87	20.87	20.87
Corn Starch	38.90	7.35	7.35	7.35	7.35	7.35
Maltodextrin 10	6.49	10.44	10.44	10.44	10.44	10.44
Sucrose	14.96	18.03	18.03	18.03	18.03	18.03
Soybean oil	2.16	2.61	2.61	2.61	2.61	2.61
Lard	1.73	18.53	18.53	18.53	18.53	18.53
L-cystine	0.26	0.31	0.31	0.31	0.31	0.31
Complex minerals S10026	0.87	1.04	1.04	1.04	1.04	1.04
Anhydrous calcium bicarbonate	1.13	1.36	1.36	1.36	1.36	1.36
calcium carbonate	0.48	0.57	0.57	0.57	0.57	0.57
Potassium citrate monohydrate	1.43	1.72	1.72	1.72	1.72	1.72
Multivitamin V10001	0.87	1.04	1.04	1.04	1.04	1.04
Choline bitartrate	0.17	0.22	0.22	0.22	0.22	0.22
Titanium dioxide	0.25	0.25	0.25	0.25	0.25	0.25
Total	100	100	100	100	100	100
Energy (kcal/g)	3.85	4.73	4.73	4.73	4.73	4.73

2.2. Chemical analyses of BSC, BSCF, YSCand YSCF

Total phenolics were quantified by Folin-Ciocalteu assay with minor adjustments (Cassani et al., 2018). Briefly, freeze-dried samples (~1.00 g) were suspended in 20 mL H_2O. Aliquots (1 mL) were reacted with 150 μL 10% Folin-Ciocalteu reagent (3 min, dark), followed by 120 μL Na_2CO_3 (75 g/L; 2 h, dark). A_{765} was measured (Tecan Infinite 200 PRO) and expressed as gallic acid equivalents (GAE). Total flavonoids were quantified via aluminum chloride assay (Cassani et al., 2018). A_{510} was measured (Tecan Infinite 200 PRO) and expressed as rutin equivalents (RE). The total anthocyanin content in the samples was determined using the spectrophotometric pH differential method (Muceniece et al., 2019; Zhang et al., 2022), and results were expressed as cyanidin-3-O-glucoside equivalents (C3G). Protein content was determined by Bradford method (Bradford, 1976). Concentrations were calculated from a bovine serum albumin (BSA) standard curve (0-1000 μg/mL)

Monosaccharide composition of BSC, YSC, BSCF, and YSCF was determined by high-performance anion-exchange chromatography coupled with pulsed amperometric detection (HPAEC-PAD) after acid hydrolysis. Samples (~13 mg) underwent pre-hydrolysis with 0.45 mL 72% H_2SO_4 (30°C, 1 h, ice bath), followed by dilution with 4.95 mL H_2O and hydrolysis (100°C, 3 h) (Chen et al., 2023; Wang et al., 2024). The hydrolyzed sample was neutralized to pH 7.0 with sodium hydroxide, then centrifuged (7100 ×g, 10 min) and filtered through a 0.22 μm membrane. After cooling, hydrolysates were diluted 4-fold and analyzed via HPAEC-PAD (Carbopac PA-1 column) with monosaccharide standards (Liu et al., 2021). The total carbohydrate content was calculated as the sum of all measured monosaccharides.

2.3. Animals and experimental design

Six-week-old male C57BL/6J mice (16–20 g; Guangdong Medical Laboratory Animal Center) were acclimated for one week under controlled conditions (23 ± 2°C, 12 h light–dark cycle) with free access to food and water. Following IACUC approval (Jinan University, #20161102111941), the animals were randomly assigned to six dietary groups (n = 8 per group) aforementioned.

Body weight was recorded weekly throughout the 14-week intervention. After an overnight fast, mice were anesthetized for retro-orbital blood collection and subsequently euthanized. The liver and adipose tissues (perirenal, epididymal, subcutaneous, and brown) were dissected and weighed. The colonic contents were collected and immediately snap-frozen in liquid nitrogen and stored at −80°C for further analysis.

2.4. Biochemical analysis

Serum metabolic biomarkers were quantified using commercial assay kits. Lipid and glucose parameters, including total cholesterol (TC), triglycerides (TG), LDL-cholesterol (LDL-C), HDL-cholesterol (HDL-C) and glucose (Glc) were measured using enzymatic kits (Nanjing Jiancheng Bioengineering Institute). Peptide YY (PYY), leptin and total bilirubin (TBIL) were determined by ELISA (Wuhan Moshake Biotechnology). All measurements were performed in accordance with the manufacturers' instructions.

2.5. Histological analysis

Liver and epididymal adipose tissues were fixed in 4% paraformaldehyde, paraffin-embedded, and sectioned (8-10 μm) for hematoxylin and eosin (H&E) staining. Frozen liver sections were stained with Oil Red O to visualize lipid accumulation. All slides were examined under an Olympus BX53 microscope. Subsequently, the images were scrutinized and assessed for the analysis of pathological changes.

2.6. Quantification of liver gene expression

Mouse liver RNA was extracted with TRIzol® (Invitrogen) and reverse-transcribed using SuperScript™ III (Invitrogen). qPCR reactions (SYBR™ Green, Applied Biosystems) were performed in triplicate with primers targeting lipid metabolism (*CPT1A, PPARA, FASN*) and inflammation genes (*TNF, IL1B, IL6, IL17A*; Table 2). Although these primers were originally designed for human sequences, they were applied to mouse liver cDNA and yielded specific amplification products with clear melt curves. Data were normalized to β-actin (*ACTB*), validated by melt curves, and analyzed via $2^{-\Delta\Delta CT}$.

2.7. 16S rRNA high-throughput sequence analysis

Six out of eight colonic content samples were randomly selected for 16S rRNA sequencing to analyze gut microbiota composition. Genomic DNA was extracted, quality-checked (NanoDrop and agarose gel), and diluted to 1 ng/μL. The V3–V4 region of the bacterial 16S rRNA gene was amplified using barcoded primers 343F/798R and KAPA HiFi Hot Start polymerase. After dual AMPure XP bead purification and Qubit quantification, equimolar amplicon pools were prepared for Illumina sequencing (Ai et al., 2022; Wang et al., 2023). The 16S rRNA gene sequencing data were processed following a standard bioinformatics pipeline. Raw FASTQ reads were quality-filtered to remove adapters, low-quality bases, and short reads, and the paired-end reads were merged after quality control. Chimeric sequences were identified and removed. High-quality reads were clustered into operational taxonomic units (OTUs) at 97% similarity using Vsearch (Rognes et al., 2016). Representative sequences were taxonomically assigned using the Silva database (version 123) and RDP classifier, and annotations with confidence values above 0.7 were retained (Wang et al., 2007). All procedures were conducted with technical support from Oebiotech Co., Ltd. (Shanghai, China).

2.8. Statistical analysis

Statistical analyses used GraphPad Prism 9.5. Normality was assessed via Kolmogorov-Smirnov test. Normally distributed data are expressed as mean ± SD and compared by one-way ANOVA; nonparametric data were analyzed with Mann-Whitney U test. Microbial composition differences were evaluated using Wilcoxon test, with covariates considered significant at $P < 0.05$. Spearman correlation assessed relationships between gut microbiota and metabolic parameters ($P < 0.05$ significance threshold).

Table 2
The inflammation of primers for qPCR.

Gene name	Primer sequences (5'-3')
IL6	Forward: TGTTAGGAGAGCATTGGA Reverse: CTGGAGTACCATAGCTACC
IL1B	Forward: AGCTCATATGGGTCCGACA Reverse: GGATGAGGACATGAGCACCT
IL17A	Forward: AGCTTTCCCTCCGCATTGACACAG Reverse: CTCCAGAAGGCCCTCAGACTAC
TNF	Forward: GAGTAGACAAGGTACAACCC Reverse: ACCCTCACACTCAGATCATC
CPT1A	Forward: CATCCACGCCATACTGCT Reverse: GACCTTGAAGTAACGGCCTC
FASN	Forward: GCTGCGGAAACTTCAGGAAAT Reverse AGAGACGTGTCACTCCTGGACTT
PPARA	Forward: TCATCAAGAAGACCGAGTCC Reverse: CCTCTTCATCCCCAAGCGTA
ACTB	Forward: TCCATACCCAAGAAGGAAGG Reverse: TGCGTGACATCAAAGAGAAG

3. Results

3.1. Compositional analysis and pectin-related monosaccharide characteristics of soybean seed coat samples

The overall chemical composition and monosaccharide profiles of BSC, BSCF, YSC, and YSCF are summarized in Table 3. BSC contained significantly higher levels of total phenolics (54.7 ± 4.3 g GAE/kg) and flavonoids (14.7 ± 6.6 g RE/kg) compared with YSC (48.8 ± 3.3 g GAE/kg and 6.4 ± 1.3 g RE/kg, respectively). Anthocyanins were detected exclusively in BSC (13.9 ± 1.3 g C3G/kg), consistent with the characteristic pigmentation of black soybean seed coats. As expected, all phenolic compounds—including anthocyanins and flavonoids—were absent in the DF-enriched fractions (BSCF and YSCF), confirming the effectiveness of the extraction procedure. Protein contents ranged from 86.5 to 107.7 g/kg, with BSCF exhibiting the highest level. Carbohydrates constituted the major component of all samples (803–841 g/kg), and YSCF contained the highest total carbohydrate content (841.5 ± 6.9 g/kg), followed by BSCF (832.1 ± 11.9 g/kg). Monosaccharide profiling revealed notable differences among samples. Glucose was the predominant sugar in all groups, particularly in BSCF (54.3 mol%). Arabinose and galactose, two hallmark units of plant pectic polysaccharide side chains, were abundant across all samples, with BSC containing the highest galactose (10.6 mol%) and YSCF containing the highest arabinose proportion (21.4 mol%). Rhamnose and galacturonic acid, both characteristic of rhamnogalacturonan domains, were consistently detected across all samples, with rhamnose present in relatively low amounts.

3.2. Soybean seed coat fibers attenuate HFD-induced weight gain and fat accumulation

Fig. 1 shows the effects of BSC, BSCF, YSC, and YSCF supplementation on body weight and adipose tissue accumulation in HFD-fed mice. As shown in Fig. 1A, mice in the HFD group displayed a continuous increase in body weight throughout the 14-week period, whereas all four intervention groups exhibited a slower rate of weight gain. At week 14 (Fig. 1B), the HFD group had significantly higher body weight than

Table 3
Overall chemical composition and monosaccharide profiles of soybean seed preparations.

Content	BSC	BSCF	YSC	YSCF
Total phenol (g GAE/kg)	54.7±4.3	nd	48.8 ±3.3	nd
Total anthocyanin content (g C3G/kg)	13.9±1.3	nd	nd	nd
Total flavonoid (g RE/kg)	14.7±6.6	nd	6.4±1.3	nd
Total protein (g/kg)	89.3±6.8	107.7 ±1.4	86.5 ±3.2	97.1 ±4.0
Total carbohydrates (g/kg)	803.1 ±10.3	832.1 ±11.9	815.8 ±8.3	841.5 ±6.9
Constituent monosaccharide (mol%)				
Glucose	47.2	54.3	43.4	42.7
Arabinose	18.0	14.6	20.8	21.4
Mannose	11.7	9.8	11.4	11.7
Galactose	10.6	9.4	9.6	8.9
Glacturonic acid	8.7	9.7	10.2	10.4
Rhamnose	2.1	1.1	2.9	2.8
Fucose	1.7	1.2	1.8	2.1

nd: not detected

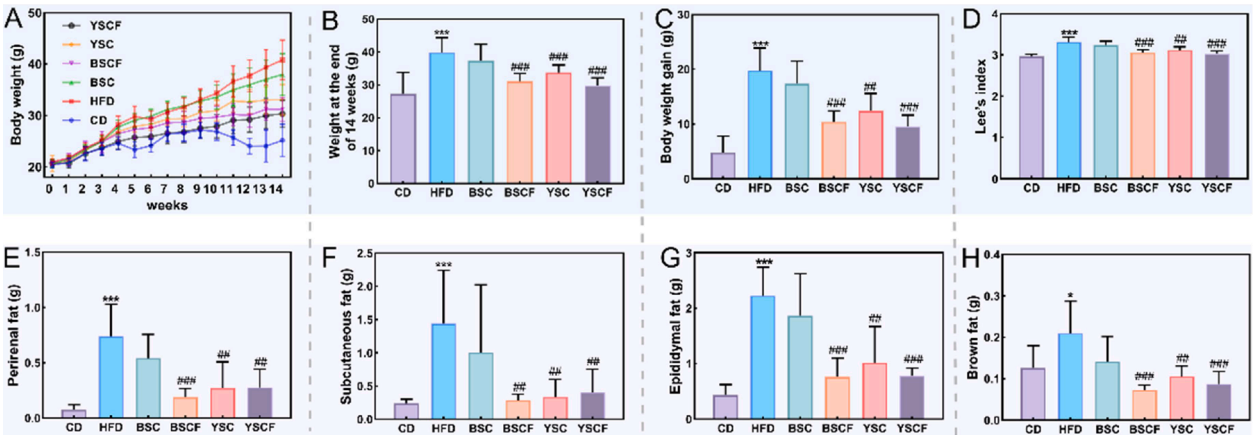

Fig. 1. Effects of BSC, BSCF, YSC, and YSCF on body weight and adipose tissue accumulation in HFD-induced obese mice. (A) Body weight during the 14-week intervention; (B) body weight at week 14; (C) body weight gain; (D) Lee's index; (E) perirenal fat mass; (F) subcutaneous fat mass; (G) epididymal fat mass; (H) brown fat mass. Data are presented as mean ± SD (n = 8). $^{*}P < 0.05$, $^{***}P < 0.001$ vs. CD group; $\#\#P < 0.01$, $\#\#\#P < 0.001$ vs. HFD group.

the CD group, while the BSCF, YSC, and YSCF groups showed significantly lower final body weights compared with the HFD group. Body weight gain (Fig. 1C) followed a similar pattern, with HFD mice gaining the most weight and BSCF, YSC, and YSCF showing significantly reduced weight gain relative to HFD. Lee's index (Fig. 1D) was also elevated in the HFD group compared with the CD group. Supplementation with BSCF, YSC, and YSCF resulted in significantly lower Lee's index values compared with the HFD group. The BSC group showed a slight reduction but did not differ significantly from HFD.

Analysis of adipose tissue mass showed that perirenal fat (Fig. 1E), subcutaneous fat (Fig. 1F), epididymal fat (Fig. 1G), and brown fat (Fig. 1H) were all higher in the HFD group relative to the CD group. In contrast, mice receiving BSCF, YSC, or YSCF had significantly lower masses of these fat depots compared with HFD. The BSC group displayed a reduction trend across all fat depots, although the differences were not statistically significant.

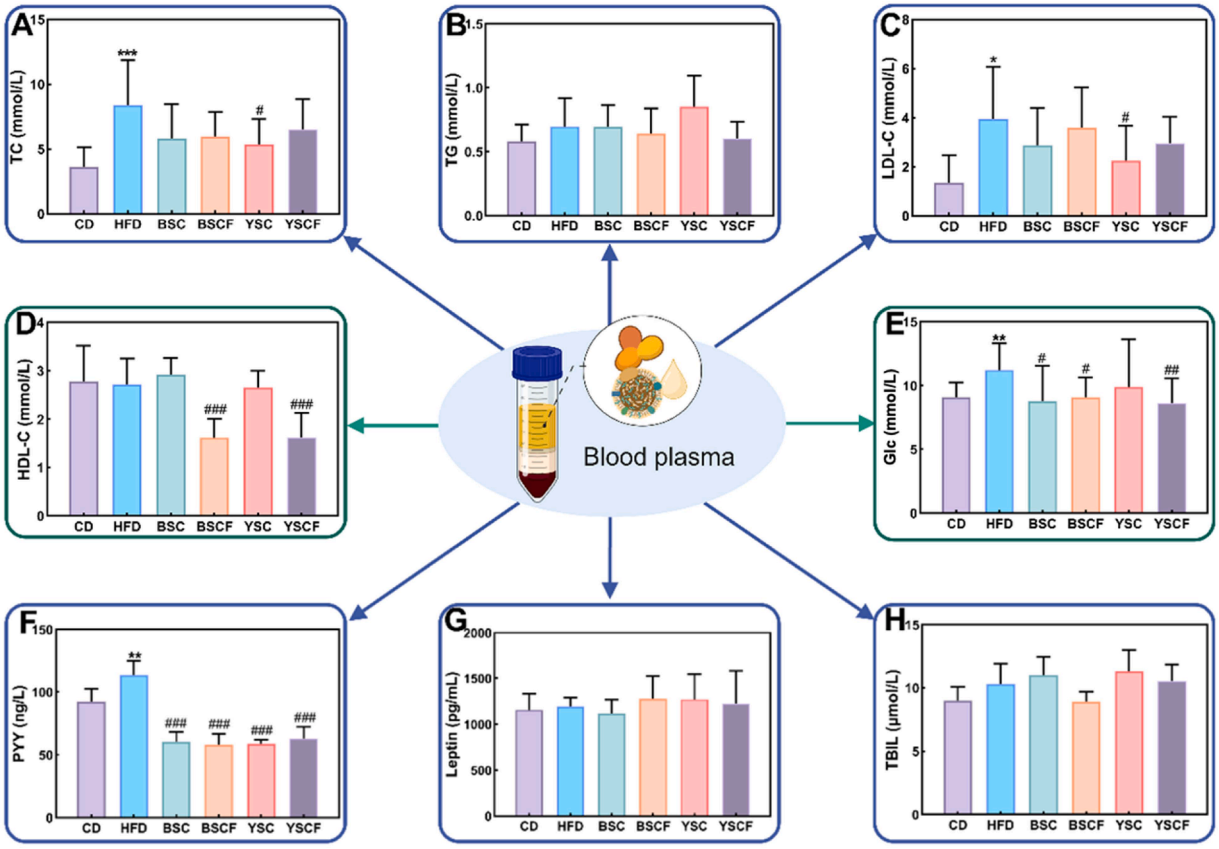

Fig. 2. Effects of BSC, BSCF, YSC, and YSCF on serum biochemical parameters in HFD-induced obese mice. (A) Total cholesterol (TC); (B) triglycerides (TG); (C) LDL-cholesterol (LDL-C); (D) HDL-cholesterol (HDL-C); (E) glucose (Glc); (F) peptide YY (PYY); (G) leptin; (H) total bilirubin (TBIL). Data are presented as mean ± SD (n = 8). $^{*}P < 0.05$, $^{**}P < 0.01$, $^{***}P < 0.001$ vs. CD group; $\#P < 0.05$, $\#\#P < 0.01$, $\#\#\#P < 0.001$ vs. HFD group.

3.3. Effects of BSC, BSCF, YSC, and YSCF on serum biochemical parameters

Fig. 2 presents the effects of BSC, BSCF, YSC, and YSCF on serum biochemical indicators in HFD-fed mice. As shown in Fig. 2A, serum TC levels were elevated in the HFD group relative to the CD group. YSC supplementation led to a significant reduction in TC compared with HFD, whereas the other interventions showed no significant changes. Serum TG (Fig. 2B) did not differ significantly among groups. LDL-C levels (Fig. 2C) increased in the HFD group compared with CD. Both YSC and YSCF produced a significant decrease in LDL-C, while BSC and BSCF showed no significant effect. In contrast, HDL-C levels (Fig. 2D) were significantly reduced by BSCF and YSCF compared with the HFD group.

Serum glucose (Fig. 2E) increased in the HFD group relative to CD, and both BSCF and YSCF significantly lowered glucose levels compared with HFD. PYY concentrations (Fig. 2F) were elevated in HFD mice; all four interventions reduced PYY, with the strongest reductions observed in YSC and YSCF. Leptin levels (Fig. 2G) showed no significant differences among groups. TBIL levels (Fig. 2H) also remained unchanged across all treatments.

3.4. Modulation of hepatic steatosis and adipocyte morphology by soybean seed coat fibers

Fig. 3 shows representative histological images of liver and epididymal adipose tissue from each treatment group. In the liver (Fig. 3A), HFD-fed mice displayed marked lipid accumulation and hepatocellular enlargement compared with the CD group. In contrast, the BSC, BSCF, YSC, and YSCF groups showed visibly reduced hepatic lipid deposition, with fewer and smaller vacuolated areas. Oil Red O staining (Fig. 3B) further confirmed these differences. The HFD group exhibited extensive lipid droplet accumulation, whereas the intervention groups displayed noticeably lower levels of lipid staining, with the greatest reduction observed in the BSCF and YSCF groups. Epididymal adipose tissue morphology is shown in Fig. 3C. Compared with the CD group, adipocytes in the HFD group were markedly enlarged. All four soybean seed coat treatments resulted in smaller adipocyte sizes relative to the HFD group, with BSCF and YSCF showing the most pronounced reduction in cell diameter.

3.5. Modulation of inflammation- and lipid metabolism–related transcriptional signals

The relative transcription-related signals of inflammation- and lipid metabolism–associated targets are shown in Fig. 4. Among inflammatory markers (Fig. 4A–D), the HFD group showed a tendency toward higher *IL6* related signal compared with the CD group. In contrast, *IL1B* and *IL17A*-related signals were reduced in the HFD group, while *TNF*-related signal remained largely unchanged between CD and HFD. Notably, all four soybean seed coat interventions reduced *IL6*-related signal and increased *IL17A*-related signal compared with the HFD group. For lipid metabolism–associated targets (Fig. 4E–G), *CPT1A* and *FASN* related signal was markedly reduced under HFD feeding, while *PPARA* related signals remained largely comparable between CD and HFD. Supplementation with soybean seed coat products modulated these transcription-related patterns, with significantly elevated *FASN*-related level in the BSCF and YSCF groups.

Correlation analysis (Fig. 4H) illustrated the relationships between inflammatory cytokines and lipid metabolism–related transcriptional signals across treatment groups. *IL1B* related signal showed a significant positive correlation with *PPARA* signal, and*IL17A* signal was strongly positively correlated with *FASN* signal. Based on the collective findings described above, a schematic model summarizing the associations between obesity-induced fatty liver and changes in hepatic inflammatory and lipid metabolism–related transcriptional signals is presented in Fig. 4I.

3.6. Modulation of gut microbial diversity and community structure by soybean seed coat fibers

The impact of HFD, BSC, BSCF, YSC and YSCF on the gut microbiota composition was further explored through high-throughput sequencing analysis of bacterial 16S rRNA genes (Fig. 5). All four soybean seed coat samples tended to increase gut microbiota richness compared to the HFD group, with BSCF showing the highest Chao1 value ($P < 0.05$) (Fig. 5A). Principal component analysis (Fig. 5B) demonstrated clear separation between the CD and HFD groups. The microbial profiles of the BSC, BSCF, YSC, and YSCF groups were distinct from that of the HFD group, and BSCF showed the greatest separation from HFD in PCA space.

At the phylum level (Fig. 5C), Firmicutes and Bacteroidetes were the dominant taxa across all groups. Compared with the CD group, the HFD group exhibited a relative increase in Firmicutes and a decrease in

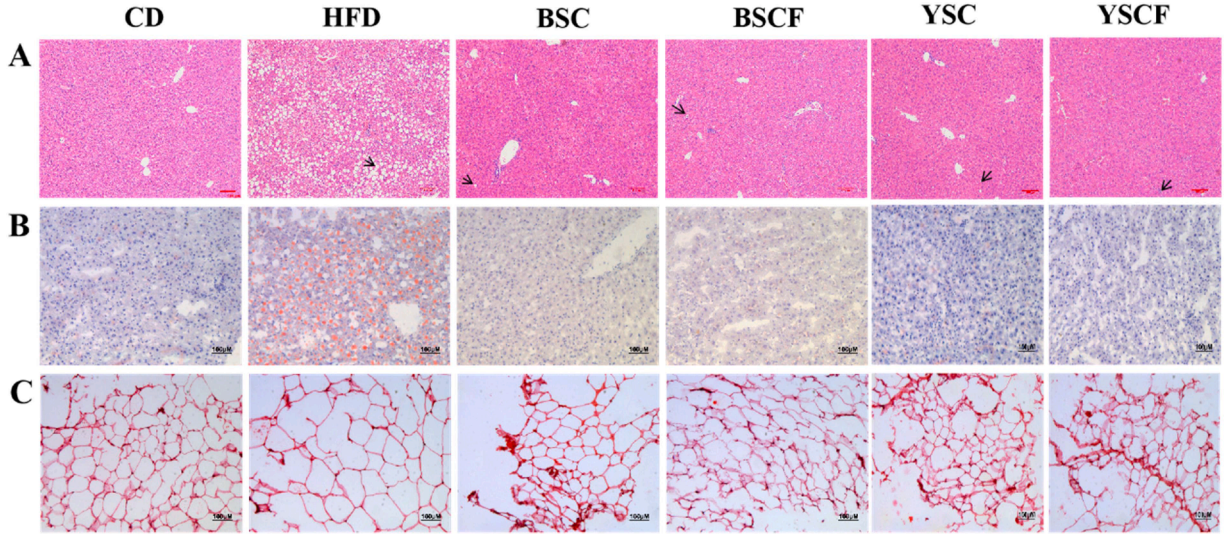

Fig. 3. Effects of BSC, BSCF, YSC, and YSCF on liver and epididymal adipose tissue morphology in HFD-induced obese mice. (A) Hematoxylin and eosin (H&E) staining of liver tissue; (B) Oil Red O staining of hepatic lipid deposition; (C) H&E staining of epididymal adipose tissue. All images were captured at 100× magnification.

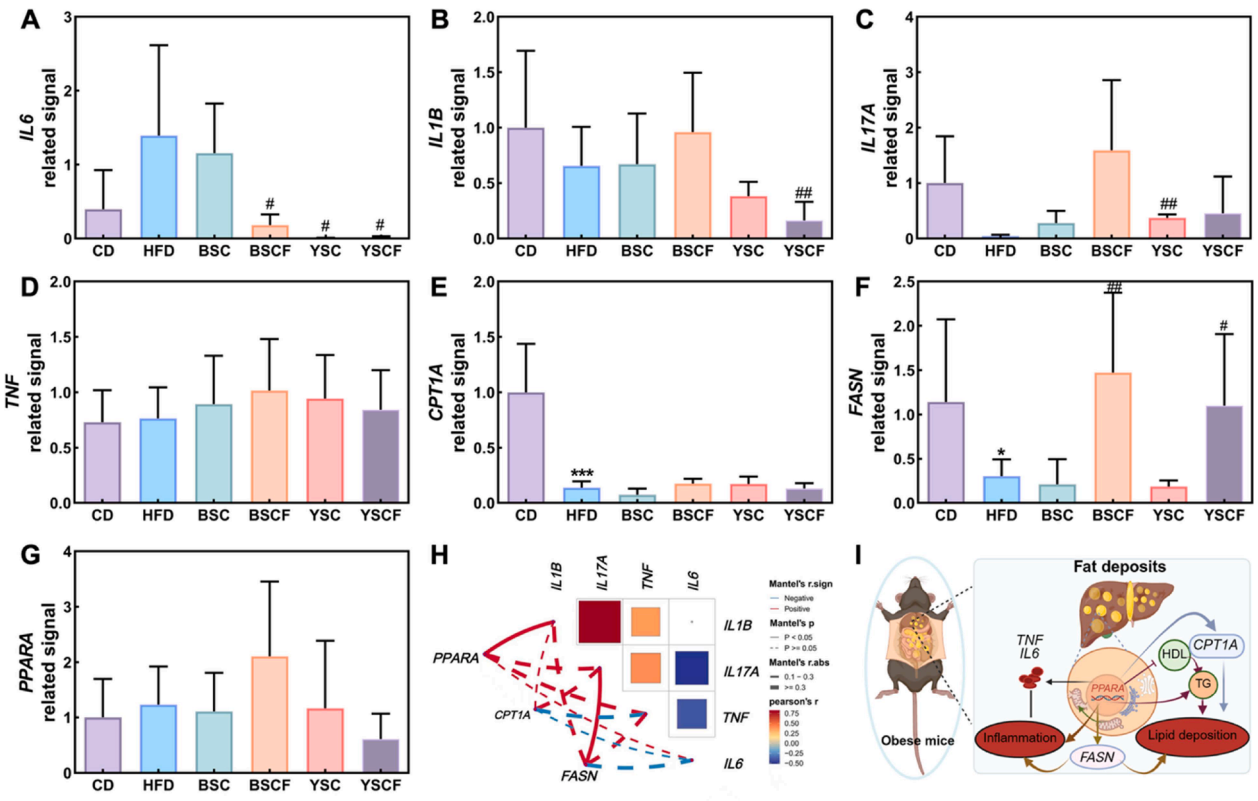

Fig. 4. Effects of BSC, BSCF, YSC, and YSCF on hepatic expression of genes related to inflammation and lipid metabolism in HFD-induced obese mice. (A) *IL6*; (B) *IL1B*; (C) *IL17A*; (D) *TNF*; (E) *CPT1A*; (F) *FASN*; (G) *PPARA*; (H) correlation analysis among inflammation- and lipid metabolism–related genes; (I) schematic representation of potential interactions between obesity-induced fatty liver, inflammation, and metabolic alterations. Data are presented as mean ± SD (n = 8). $^{*}P < 0.05$, $^{***}P < 0.001$ vs. CD group; $\#P < 0.05$, $\#\#P < 0.01$ vs. HFD group.

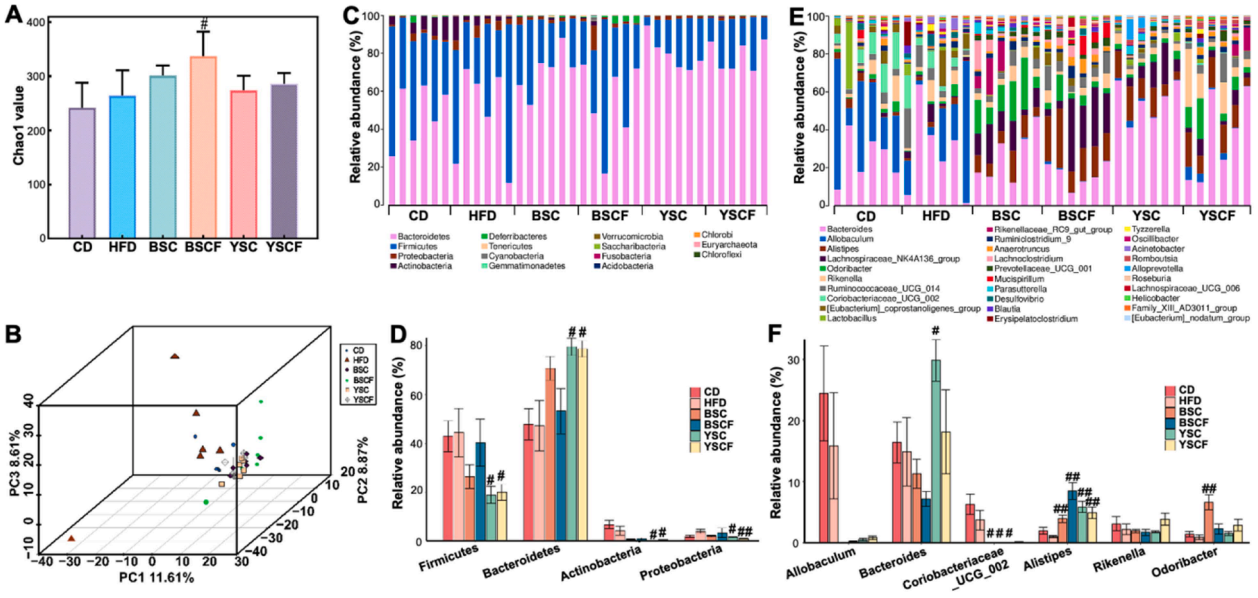

Fig. 5. Effects of BSC, BSCF, YSC, and YSCF on gut microbiota diversity and composition in HFD-induced obese mice. (A) α-diversity assessed by the Chao1 index; (B) β-diversity analysis based on principal component analysis (PCA); (C) Relative abundance of gut microbiota at the phylum level; (D) Relative abundance of gut microbiota at the genus level; (E) Relative abundance of selected dominant phyla; (F) Relative abundance of selected dominant genera. Data are presented as mean ± SD (n = 6). $\#P < 0.05$, $\#\#P < 0.01$ *vs.* HFD group.

Bacteroidetes. Supplementation with BSC, BSCF, YSC, or YSCF partially altered this distribution, resulting in a lower Firmicutes-to-Bacteroidetes ratio compared with HFD. In comparison to the HFD group, YSC and YSCF reduced the abundance of Actinobacteria and Proteobacteria compared with HFD group ($P < 0.05$), BSC and BSCF showed similar effects, although this was not statistically significant ($P > 0.05$) (Fig. 5D). The study delved deeper into the analysis of gut microbiota at the genus level (Fig. 5E). Compared with CD group, HFD was found to

diminish the abundance of *Allobaculum,Bacteroides,Coriobacteriaceae_UCG_002,Alistipes, Rikenella and Odoribacter,* although it was not statistically significant ($P > 0.05$) (Fig. 5F). The relative abundance of *Alistipes* was significantly ($P < 0.01$) higher in the seed coat–supplemented groups than in the HFD group, with BSCF showing the most pronounced increase. Compared with HFD group, YSC significantly ($P < 0.05$) elevated the relative abundance of *Bacteroides* and the relative abundance of *Odoribacter* was significantly ($P < 0.01$) increased by BSC (Fig. 5F).

3.7. Correlation analysis between gut microbiota and host parameters

Spearman correlation analysis identified several significant associations between gut microbial taxa and host-related metabolic and inflammatory indicators (Fig. 6). Several genera showed significant positive correlations with PYY levels and brown fat weights, including *Lactobacillus* ($P < 0.01$), *Allobaculum* ($P < 0.05$) and *Coriobacteriaceae_UCG_002* ($P < 0.01$). *Alistipes* was positively correlated with *IL17A* related signal ($P < 0.05$), while showing negative correlations with PYY level ($P < 0.01$), brown fat weight ($P < 0.01$), HDL-C level ($P < 0.01$) and *IL6* related signal ($P < 0.05$). *Bacteroides* was negatively correlated with *PPARA* and *IL6* related signals ($P < 0.01$), and epididymal fat weights ($P < 0.05$)

4. Discussion

Soybean seed coats, which constitute the protective testa surrounding the cotyledons, are generated in large quantities during the processing of whole soybeans. Unlike soybean pod hulls, seed coats possess a unique cell-wall architecture enriched in pectin-related polysaccharides and phenolic compounds. The present study demonstrates that both black and yellow soybean seed coats contain high levels (> 803.1 g/kg) of carbohydrates, dominated by cellulose and polysaccharides rich in arabinose, galactose, rhamnose, and galacturonic acid—structural hallmarks of pectin and rhamnogalacturonan I (RG-I) (Yüksel et al., 2025). Removal of extractable flavonoids further enriched the polysaccharide fraction, yielding BSCF and YSCF with even higher carbohydrate content and clearer pectin signatures. These compositional features establish soybean seed coat fiber as a pectin-containing matrix and provide a basis for its physiological activity.

To achieve physiologically relevant pectin levels in the diet, relatively high amounts of seed coat material were incorporated into the experimental formulations. Consequently, the CD also contained elevated cellulose to maintain DF parity across groups. High-DF diets are known to modestly reduce energy intake and slow weight gain in rodents (McCay et al., 1934; Zhai et al., 2018), which is consistent with our observation that CD mice gained weight more slowly compared with typical normal chow-fed controls (data not shown). However, the DF composition differed fundamentally between the CD and intervention groups. Cellulose is a poorly fermentable, non-viscous insoluble DF, whereas soybean seed coats supply pectin-rich, partially soluble, and fermentable polysaccharides with well-documented functional effects on digestion, lipid absorption, and microbiota metabolism (Gunness & Gidley, 2010; Mullin & Xu, 2000; Tian et al., 2017; Tian et al., 2019). Therefore, the metabolic improvements observed in the BSC-, BSCF-, YSC-, and YSCF-fed groups reflect qualitative differences in fine structure, not DF quantity.

In line with this distinction, dietary supplementation with seed coat materials markedly attenuated HFD-induced obesity. Significant reductions were observed in body weight gain, Lee's index, and multiple adipose depots. These effects are consistent with known physiological functions of soluble DFs and pectins, which can increase digesta viscosity, delay gastric emptying, reduce nutrient absorption, and enhance satiety signaling (Ciriminna et al., 2022; Morell et al., 2014; Pirsa & Hafezi, 2023). Pectin's ability to form viscous gels in the gastrointestinal tract is strongly associated with reduced energy intake and improved postprandial lipid metabolism (Song et al., 2024). The enhanced effects observed in the DF-enriched fractions indicate that the pectin

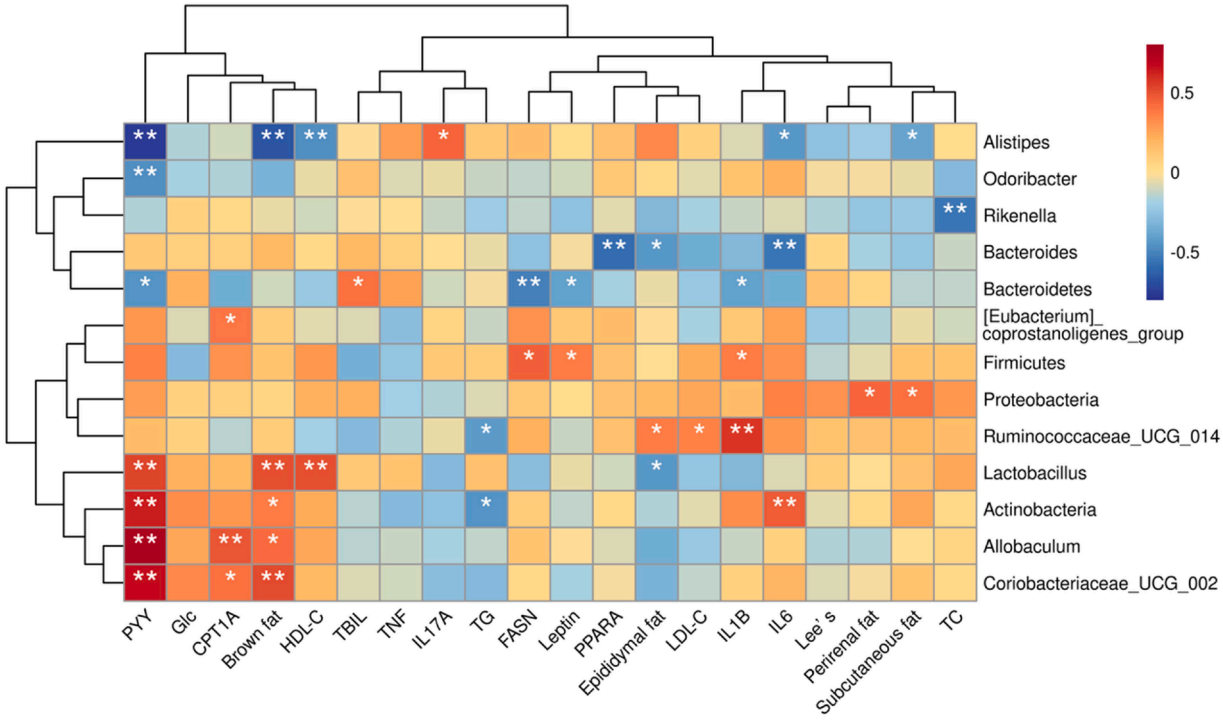

Fig. 6. Spearman correlation heatmap between selected gut microbiota and host-related indicators in CD-, HFD-, and soybean seed coat–treated mice. The heatmap displays correlation coefficients between microbial taxa (rows) and host parameters (columns), including hepatic gene expression, serum biochemical indicators, and adiposity-related traits such as fat depot weight and Lee's index. Positive and negative correlations are shown in red and blue, respectively. Asterisks indicate statistical significance ($P < 0.05$, $P < 0.01$). Variables were hierarchically clustered based on correlation profiles.

component of seed coats is a primary contributor to these physiological improvements.

Serum biochemical analysis further highlighted the metabolic benefits of seed coat supplementation. Several treatments reduced serum TC, LDL-C, and glucose concentrations relative to HFD controls. Such improvements parallel findings that pectin can bind bile acids, alter micelle formation, and modify lipid absorption, thereby lowering circulating cholesterol (Brouns et al., 2012; Gunness & Gidley, 2010; Song et al., 2024). Reductions in serum PYY observed in supplemented groups may reflect decreased energy intake and adiposity, consistent with studies showing that weight loss and improved metabolic status are associated with normalization of satiety hormone levels (Batterham et al., 2006; Fernandes et al., 2020). Although TG and leptin showed modest changes, the overall biochemical profile supports improved metabolic regulation.

Histological and molecular analyses revealed that soybean seed coat supplementation mitigated hepatic steatosis and inflammation. HFD-induced lipid accumulation in hepatocytes was markedly reduced, particularly in the BSCF and YSCF groups. Obesity is characterized by the enlargement of individual adipocytes and adipose tissue (McNelis & Olefsky, 2014). This observation was confirmed by the enlargement of fat cells seen in HFD mice during HE staining in this study. BSC, BSCF, YSC, and YSCF effectively hindered the enlargement of adipocytes in obese mice. This could be achieved by inhibiting adipocyte differentiation and abnormal lipid metabolism (Kwon et al., 2007).

In obesity, adipose tissue is widely recognized to secrete pro-inflammatory mediators such as IL-6, IL-1β and TNF-α, which contribute to chronic low-grade inflammation and exacerbate adipocyte hypertrophy and hepatic lipid deposition (Hotamisligil, 2017; Ouchi et al., 2011). In our study, however, not all inflammation-related transcriptional signals followed the expected HFD-induced elevation. While *IL6* showed modest increases in HFD mice and were partially reduced by BSCF, YSC, and YSCF supplementation, *IL1B* and *TNF* did not display significant HFD-induced upregulation. This could be partly explained by the compensatory cytokine responses after a long-term HFD feeding. IL-17, in particular, has been reported to inhibit adipogenesis (Shin et al., 2009), and its restoration in the treatment groups may reflect a shift toward a less lipogenic hepatic milieu. In addition, the counterintuitive pattern of *FASN* signal may be attributed to the fact that high-fat diets often suppress hepatic de novo lipogenesis, as exogenous fatty acids become the predominant substrate for triglyceride accumulation (Morigny et al., 2021). Notably, the partial normalization of hepatic gene expression in the DF-supplemented groups suggests that soybean seed coat DFs may help maintain a more balanced inflammatory environment and lipid metabolism.

Intestinal dysbiosis is now recognized as a major factor contributing to the development and progression of obesity (Everard et al., 2011). Gut microbiota analysis showed that seed coat supplementation partially restored HFD-induced microbial dysbiosis. β-diversity analysis revealed distinct clustering of the four intervention groups away from the HFD group, indicating substantial restructuring of the gut microbial community. The seed coat preparations reduced the Firmicutes-to-Bacteroidetes ratio and the abundance of Proteobacteria, suggesting a potential role of soybean seed coat pectin in mitigating obesity-associated dysbiosis (Zou et al., 2018). *Alistipes*, a genus generally enriched in metabolically healthy individuals (Xu et al., 2013), showed increased abundance in all seed coat treatment groups, with BSCF inducing the greatest restoration. This pattern suggests that seed coat fibers, particularly their DF-enriched fractions, may promote the recovery of taxa linked to improved metabolic function. The inverse correlation observed between *Alistipes* abundance and hepatic *IL6* related signal in our analysis further supports its potential role in attenuating inflammation. While *Bacteroides* species are known for their capacity to degrade complex polysaccharides and generate SCFAs (Luis et al., 2018), some strains may also attenuate host inflammatory responses and hepatic lipid deposition (Wang et al., 2021). Its enrichment in the soybean DF-supplemented groups may reflect enhanced microbial fermentation and reduced HFD-induced dysbiosis. The inverse association with *IL6* is consistent with previous studies highlighting the anti-inflammatory potential of *Bacteroides*, likely through SCFA-mediated immune modulation (Wang et al., 2021). The concurrent negative correlation with *PPARA*, a key regulator of fatty acid oxidation, may reflect reduced hepatic metabolic stress and lipid burden under fiber-rich interventions, possibly leading to a transient down-regulation of oxidative pathways. Although *Lactobacillus* abundance did not differ significantly across treatment groups, its relative levels were positively correlated with PYY levels and brown fat weight. This suggests that even modest inter-individual variation in *Lactobacillus* may be functionally relevant in shaping host metabolic responses. Previous studies have linked *Lactobacillus* species to improved satiety hormone secretion, thermogenesis, and SCFA production (Sun et al., 2025), supporting a potential role in host energy regulation.

5. Conclusion

This study demonstrates that soybean seed coats, an underutilized byproduct of soybean processing, are a rich source of pectin-like polysaccharides with significant physiological benefits. Both black and yellow seed coats contained high levels of arabinose-, galactose-, rhamnose-, and galacturonic acid–rich polysaccharides characteristic of rhamnogalacturonan-I structures. Dietary supplementation with seed coat preparations effectively attenuated multiple features of HFD-induced obesity, including body weight gain, adiposity, hepatic steatosis, and selected serum metabolic disturbances. Improvements in inflammatory and lipid-metabolism-related gene expression, together with histological protection of liver and adipose tissues, highlight the metabolic bioactivity of these DFs. In addition, soybean seed coat supplementation reshaped gut microbiota composition by increasing α-diversity, modulating key phyla and genera associated with metabolic health, and reducing taxa linked to inflammation. Overall, these findings indicate that soybean seed coats, especially their DF-enriched fractions, represent a promising new source of pectin-rich hydrocolloids with potential applications in functional foods targeting obesity and metabolic disorders.

Fundings

This work was supported by the National Key Research and Development Program of China (2024YFD2101301 under Grant 2024YFD2101300), the National Natural Science Foundation of China (32272334), the Natural Science Foundation of Guangdong Province (2023A1515012281), and the Fundamental Research Funds for the Central Universities (21624112).

Ethical statement

This study was approved by the Animal Care and Use Committee (IACUC) of Jinan University, Protocol #20161102111941, in compliance with national guidelines.

CRediT authorship contribution statement

Xiaoyi Liu: Writing – original draft, Visualization, Formal analysis. **Guowei Chen:** Writing – original draft, Visualization, Investigation, Formal analysis, Data curation. **Junliang Chen:** Investigation, Formal analysis. **Jiahong Huo:** Formal analysis. **Hong Yao:** Writing – review & editing, Supervision. **Maurizio Battino:** Writing – review & editing. **Weibin Bai:** Writing – review & editing, Supervision, Conceptualization. **Lingmin Tian:** Writing – review & editing, Supervision, Project administration, Conceptualization.

Declaration of competing interest

The authors declare no potential conflict of interests.

Data availability

Data will be made available on request.

References

Ai, J., Yang, Z., Liu, J., Schols, H. A., Battino, M., Bao, B., Tian, L., & Bai, W. (2022). Structural characterization and in vitro fermentation characteristics of enzymatically extracted black mulberry polysaccharides. *Journal of Agricultural and Food Chemistry, 70*, 3654–3665. https://doi.org/10.1021/acs.jafc.1c07810

Batterham, R. L., Heffron, H., Kapoor, S., Chivers, J. E., Chandarana, K., Herzog, H., Le Roux, C. W., Thomas, E. L., Bell, J. D., & Withers, D. J. (2006). Critical role for peptide YY in protein-mediated satiation and body-weight regulation. *Cell Metabolism, 4*, 223–233. https://doi.org/10.1016/j.cmet.2006.08.001

Bradford, M. M. (1976). A rapid and sensitive method for the quantitation of microgram quantities of protein utilizing the principle of protein-dye binding. *Analytical Biochemistry, 72*, 248–254. https://doi.org/10.1016/0003-2697(76)90527-3

Brouns, F., Theuwissen, E., Adam, A., Bell, M., Berger, A., & Mensink, R. P. (2012). Cholesterol-lowering properties of different pectin types in mildly hypercholesterolemic men and women. *European Journal of Clinical Nutrition, 66*, 591–599. https://doi.org/10.1038/ejcn.2011.208

Cassani, L., Gerbino, E., Moreira, M. D., & Gómez-Zavaglia, A. (2018). Influence of non-thermal processing and storage conditions on the release of health-related compounds after in vitro gastrointestinal digestion of fiber-enriched strawberry juices. *Journal of Functional Foods, 40*, 128–136. https://doi.org/10.1016/j.jff.2017.11.005

Chen, L., Wang, Y., Liu, J., Hong, Z., Wong, K. H., Chiou, J. C., Xu, B., Cespedes-Acuna, C. L., Bai, W., & Tian, L. (2023). Structural characteristics and in vitro fermentation patterns of polysaccharides from *Boletus* mushrooms. *Food & Function, 14*, 7912–7923. https://doi.org/10.1039/d3fo01085f

Cheng, Z., Zhang, L., Yang, L., & Chu, H. (2022). The critical role of gut microbiota in obesity. *Frontiers in Endocrinology, 13*, Article 1025706. https://doi.org/10.3389/fendo.2022.1025706

Ciriminna, R., Fidalgo, A., Scurria, A., Ilharco, L. M., & Pagliaro, M. (2022). Pectin: New science and forthcoming applications of the most valued hydrocolloid. *Food Hydrocolloids, 127*, Article 107483. https://doi.org/10.1016/j.foodhyd.2022.107483

Everard, A., Lazarevic, V., Derrien, M., Girard, M., Muccioli, G. G., Neyrinck, A. M., & Cani, P. D. (2011). Responses of gut microbiota and glucose and lipid metabolism to prebiotics in genetic obese and diet-induced leptin-resistant mice. *Diabetes, 60*, 2775–2786. https://doi.org/10.2337/db11-0227

Fernandes, S. P., Alessi, J., Santos, Z. E., & de Mello, E. D. (2020). Association between eating behavior, anthropometric and biochemical measurements, and peptide YY (PYY) hormone levels in obese adolescents in outpatient care. *Journal of Pediatric Endocrinology and Metabolism, 33*, 873–877. https://doi.org/10.1515/jpem-2020-0033

Gunness, P., & Gidley, M. J. (2010). Mechanisms underlying the cholesterol-lowering properties of soluble dietary fibre polysaccharides. *Food & Function, 1*, 149–155. https://doi.org/10.1039/C0FO00080A

Hironao, K. Y., Ashida, H., & Yamashita, Y. (2022). Black soybean seed coat polyphenol ameliorates the abnormal feeding pattern induced by high-fat diet consumption. *Frontiers in Nutrition, 9*, Article 1006132. https://doi.org/10.3389/fnut.2022.1006132

Hotamisligil, G. S. (2017). Inflammation, metaflammation and immunometabolic disorders. *Nature, 542*, 177–185. https://doi.org/10.1038/nature21363

Ju, Y., Huang, L., Luo, H., Huang, Y., Huang, X., Chen, G., Gui, J., Lin, S., Liu, X., & Yang, L. (2025). Passion fruit peel pectin improves glucose and lipid metabolism in high-fat diet-induced obesity through gut microbiota and insulin sensitivity regulation. *Food Bioscience, 70*, Article 107050. https://doi.org/10.1016/j.fbio.2025.107050

Kwon, S. H., Ahn, I. S., Kim, S. O., Kong, C. S., Chung, H. Y., Do, M. S., & Park, K. Y. (2007). Anti-obesity and hypolipidemic effects of black soybean anthocyanins. *Journal of Medicinal Food, 10*, 552–556. https://doi.org/10.1089/jmf.2006.147

Le Chatelier, E., Nielsen, T., Qin, J., Prifti, E., Hildebrand, F., Falony, G., & Pedersen, O. (2013). Richness of human gut microbiome correlates with metabolic markers. *Nature, 500*, 541–546. https://doi.org/10.1038/nature12506

Liu, D., Tang, W., Yin, J. Y., Nie, S. P., & Xie, M. Y. (2021). Monosaccharide composition analysis of polysaccharides from natural sources: Hydrolysis condition and detection method development. *Food Hydrocolloids, 116*, Article 106641. https://doi.org/10.1016/j.foodhyd.2021.106641

Luis, A. S., Briggs, J., Zhang, X., Farnell, B., Ndeh, D., Labourel, A., Baslé, A., Cartmell, A., Terrapon, N., Stott, K., Lowe, E. C., McLean, R., Shearer, K., Schückel, J., Venditto, I., Ralet, M. C., Henrissat, B., Martens, E. C., Mosimann, S. C., Abbott, D. W., & Gilbert, H. J. (2018). Dietary pectic glycans are degraded by coordinated enzyme pathways in human colonic *Bacteroides*. *Nature Microbiology, 3*, 210–219. https://doi.org/10.1038/s41564-017-0079-1

McNelis, J. C., & Olefsky, J. M. (2014). Macrophages, immunity, and metabolic disease. *Immunity, 41*, 36–48. https://doi.org/10.1016/j.immuni.2014.05.010

McCay, C. M., Ku, C. C., Woodward, J. C., & Sehgal, B. S. (1934). Cellulose in the diet of rats and mice: Two figures. *The Journal of Nutrition, 8*, 435–447. https://doi.org/10.1093/jn/8.4.435

Méndez-Albiñana, P., Rodrigues-Díez, R., Rodríguez-Rodríguez, P., Moreno, R., Muñoz-Valverde, D., Casani, L., Mar, V., & Blanco-Rivero, J. (2025). Structure and properties of citrus pectin as influencing factors of biomarkers of metabolic syndrome in rats fed with a high-fat diet. *Current Research in Food Science, 10*, Article 101014. https://doi.org/10.1016/j.crfs.2025.101014

Morell, P., Fiszman, S. M., Varela, P., & Hernando, I. (2014). Hydrocolloids for enhancing satiety: Relating oral digestion to rheology, structure and sensory perception. *Food Hydrocolloids, 41*, 343–353. https://doi.org/10.1016/j.foodhyd.2014.04.038

Morigny, P., Boucher, J., Arner, P., & Langin, D. (2021). Lipid and glucose metabolism in white adipocytes: Pathways, dysfunction and therapeutics. *Nature Reviews Endocrinology, 17*, 276–295. https://doi.org/10.1038/s41574-021-00471-8

Muceniece, R., Klavins, L., Kviesis, J., Jekabsons, K., Rembergs, R., Saleniece, K., Dzirkale, Z., Saulite, L., Riekstina, U., & Klavins, M. (2019). Antioxidative, hypoglycaemic and hepatoprotective properties of five *Vaccinium* spp. berry pomace extracts. *Journal of Berry Research, 9*, 267–282. https://doi.org/10.3233/JBR-180351

Mullin, W. J., & Xu, W. (2000). A study of the intervarietal differences of cotyledon and seed coat carbohydrates in soybeans. *Food Research International, 33*, 883–891. https://doi.org/10.1016/S0963-9969(00)00118-6

Ouchi, N., Parker, J. L., Lugus, J. J., & Walsh, K. (2011). Adipokines in inflammation and metabolic disease. *Nature Reviews Immunology, 11*, 85–97. https://doi.org/10.1038/nri2921

Pirsa, S., & Hafezi, K. (2023). Hydrocolloids: Structure, preparation method, and application in food industry. *Food Chemistry, 399*, Article 133967. https://doi.org/10.1016/j.foodchem.2022.133967

Rajha, H. N., Paule, A., Aragones, G., Barbosa, M., Caddeo, C., Debs, E., & Edeas, M. (2022). Recent advances in research on polyphenols: Effects on microbiota, metabolism, and health. *Molecular Nutrition & Food Research, 66*, Article e2100670. https://doi.org/10.1002/mnfr.202100670

Rognes, T., Flouri, T., Nichols, B., Quince, C., & Mahé, F. (2016). VSEARCH: A versatile open source tool for metagenomics. *PeerJ, 4*, e2584. https://doi.org/10.7717/peerj.2584

Shin, J. H., Shin, D. W., & Noh, M. (2009). Interleukin-17A inhibits adipocyte differentiation in human mesenchymal stem cells and regulates pro-inflammatory responses in adipocytes. *Biochemical Pharmacology, 77*, 1835–1844. https://doi.org/10.1016/j.bcp.2009.03.008

Song, H., Chen, F., Cao, Y., Wang, F., Wang, L., Xiong, L., & Shen, X. (2024). Innovative applications of pectin in lipid management: Mechanisms, modifications, synergies, nanocarrier systems, and safety considerations. *Journal of Agricultural and Food Chemistry, 72*, 20261–20272. https://doi.org/10.1021/acs.jafc.4c06586

Sun, Y., Li, D., Zhao, L., Liu, X., Guan, K., Ma, Y., Wang, R., & Li, Q. (2025). PYY-mediated appetite control and obesity alleviation through short-chain fatty acid–driven gut-brain axis modulation by *Lacticaseibacillus rhamnosus* HF01 isolated from Qula. *Journal of Dairy Science, 108*, 7960–7978. https://doi.org/10.3168/jds.2024-26193

Tian, L., Bruggeman, G., van den Berg, M., Borewicz, K., Scheurink, A. J., Bruininx, E., de Vos, P., Smidt, H., Schols, H. A., & Gruppen, H. (2017). Effects of pectin on fermentation characteristics, carbohydrate utilization, and microbial community composition in the gastrointestinal tract of weaning pigs. *Molecular Nutrition & Food Research, 61*, Article 1600186. https://doi.org/10.1002/mnfr.201600186

Tian, L., Scholte, J., Borewicz, K., van den Bogert, B., Smidt, H., Scheurink, A. J., Gruppen, H., & Schols, H. A. (2016). Effects of pectin supplementation on the fermentation patterns of different structural carbohydrates in rats. *Molecular Nutrition & Food Research, 60*, 2256–2266. https://doi.org/10.1002/mnfr.201600149

Tian, L., Scholte, J., Scheurink, A. J. W., van den Berg, M., Bruggeman, G., Bruininx, E., de Vos, P., Schols, H. A., & Gruppen, H. (2019). Effect of oat and soybean rich in distinct non-starch polysaccharides on fermentation, appetite regulation and fat accumulation in rat. *International Journal of Biological Macromolecules, 140*, 515–521. https://doi.org/10.1016/j.ijbiomac.2019.08.032

Wang, C., Zhao, J., Zhang, H., Lee, Y. K., Zhai, Q., & Chen, W. (2021). Roles of intestinal *bacteroides* in human health and diseases. *Critical Reviews in Food Science and Nutrition, 61*, 3518–3536. https://doi.org/10.1080/10408398.2020.1802695

Wang, Q., Garrity, G. M., Tiedje, J. M., & Cole, J. R. (2007). Naive Bayesian classifier for rapid assignment of rRNA sequences into the new bacterial taxonomy. *Applied and Environmental Microbiology, 73*, 5261–5267. https://doi.org/10.1128/AEM.00062-07

Wang, Y., Liu, J., Chen, L., Jin, S., An, C., Chen, L., Yang, B., Schols, H. A., de Vos, P., Bai, W., & Tian, L. (2023). Effects of thermal treatments on the extraction and in vitro fermentation patterns of pectins from pomelo (*Citrus grandis*). *Food Hydrocolloids, 141*, Article 108755. https://doi.org/10.1016/j.foodhyd.2023.108755

Wang, Y., Liu, J., Long, Y., Yao, H., Schols, H. A., de Vos, P., Bai, W., & Tian, L. (2024). Enzymatic modification of pomelo pectins for shaping the gut microbiota to a healthy pattern. *Food Hydrocolloids, 152*, Article 109939. https://doi.org/10.1016/j.foodhyd.2024.109939

Xu, X., So, J. S., Park, J. G., & Lee, A. H. (2013). Transcriptional control of hepatic lipid metabolism by SREBP and ChREBP. *Seminars in Liver Disease, 33*, 301–311. https://doi.org/10.1055/s-0033-1358523

Yang, J., Xiao, A., & Wang, C. (2014). Novel development and characterisation of dietary fibre from yellow soybean hulls. *Food Chemistry, 161*, 367–375. https://doi.org/10.1016/j.foodchem.2014.04.030

Yüksel, E., Voragen, A. G., & Kort, R. (2025). The pectin metabolizing capacity of the human gut microbiota. *Critical Reviews in Food Science and Nutrition, 65*, 4823–4845. https://doi.org/10.1080/10408398.2024.2400235

Zhai, X., Lin, D., Zhao, Y., Li, W., & Yang, X. (2018). Effects of dietary fiber supplementation on fatty acid metabolism and intestinal microbiota diversity in C57BL/6J mice fed with a high-fat diet. *Journal of Agricultural and Food Chemistry, 66*, 12706–12718. https://doi.org/10.1021/acs.jafc.8b05036

Zhang, W., Li, X., Ma, X., Li, H., Liu, J., Zeng, Y., Cai, D., Xu, Q., Chen, G., Tian, L., Sun, J., & Bai, W. (2024). Microencapsulation of anthocyanins extracted from black soybean peels by whey protein/fructo-oligosaccharide contributes to improved stability, bioavailability, and ability to regulate glycolipid metabolism. *Food Frontiers, 5*, 570–583. https://doi.org/10.1002/fft2.333

Zhang, X., Wang, S., Wu, Q., Battino, M., Giampieri, F., Bai, W., & Tian, L. (2022). Recovering high value-added anthocyanins from blueberry pomace with ultrasound-assisted extraction. *Food Chemistry-X, 16*, Article 100476. https://doi.org/10.1016/j.fochx.2022.100476

Zou, J., Chassaing, B., Singh, V., Pellizzon, M., Ricci, M., Fythe, M. D., Kumar, M. V., & Gewirtz, A. T. (2018). Fiber-mediated nourishment of gut microbiota protects against diet-induced obesity by restoring IL-22-mediated colonic health. *Cell Host & Microbe, 23*, 41–53. https://doi.org/10.1016/j.chom.2017.11.003